# High Nitrate Variability on an Alaskan Permafrost Hillslope Dominated by Alder Shrubs

Rachael E. McCaully[1,2], Carli A. Arendt[1,2], Brent D. Newman[1], Verity G. Salmon[3], Jeffrey M. Heikoop[1], Cathy J. Wilson[1], Sanna Sevanto[1], Nathan A. Wales[1], George B. Perkins[1], Oana C. Marina[1] and Stan D.

[1]Earth and Environmental Sciences Division, Los Alamos National Laboratory, Los Alamos, 87545, United States
[2]Department of Marine Earth and Atmospheric Sciences, North Carolina State University, Raleigh, 27695, United States
[3]Environmental Sciences Division and Climate Change Science Institute, Oak Ridge National Laboratory, Oak Ridge, 37830, United States

*Correspondence to*: Carli A. Arendt (carendt@ncsu.edu)

**Abstract.** In Arctic ecosystems, increasing temperatures are driving the expansion of nitrogen (N) fixing shrubs across tundra landscapes. The implications of this expansion to the biogeochemistry of Arctic ecosystems is of critical importance and more work is needed to better understand the form, availability, and transportation potential of N from these shrubs across a variety of Arctic landscapes. To gain insights to processes controlling N within a permafrost hillslope system, the spatiotemporal variability of nitrate ($NO_3^-$) and its environmental controls were investigated at an alder (*Alnus viridis* spp. *fruticosa*) dominated permafrost tundra landscape in the Seward Peninsula, Alaska, USA. Soil pore water was collected from locations *within* alder shrubland growing along a well-drained hillslope and compared to soil pore water collected from locations *outside (upslope, downslope, and between)* the alder shrubland. Soil pore water collected within alder shrubland had an average $NO_3$-N (nitrogen from nitrate) concentration of $4.27 \pm 8.02$ mg $L^{-1}$ and differed significantly from locations outside alder shrubland ($0.23 \pm 0.83$ mg $L^{-1}$; $p < 0.05$). Temporal variation in $NO_3$-N within and downslope of alder shrubland co-occurred with precipitation events, where $NO_3^-$ that accumulated in the soil was likely flushed downslope during rainfall. These findings have important implications for nutrient availability and mobility in N-limited permafrost systems that are experiencing shrub expansion in response to a warming Arctic.

## 1 Introduction

### 1.1 Background

Ecosystems in the Arctic are directly and continually impacted by increasing global temperatures (Martin et al., 2008; Chapin et al., 2000; McClelland et al., 2007; Hovelsrud et al., 2011; Schuur et al., 2015), including permafrost degradation with subsequent feedbacks that impact soil moisture, vegetation, and nutrient availability (Shaver and Chapin, 1980; Weintraub and Schimel, 2005; Hinzman et al., 2013; Street et al., 2015; Salmon et al., 2016; Walvoord and Kurylyk, 2016). While there is a clear relationship between climate-induced shifts in vegetation and nutrient abundance, many details remain unknown or

unpublished about the variability of nutrient availability across- and nutrient mobility within- permafrost systems (Sharkhuu and Sharkhuu, 2012; Barnes et al., 2014; Keuper et al., 2017; Rasmussen et al., 2020; Rasmussen et al., 2022).

35

In landscapes with a topographic gradient, $NO_3^-$ contributions in upland areas to surface waters can impact downslope hydrochemistry and alter downstream ecosystems (Vitousek et al., 1997; Koch et al., 2013; Hiltbrunner et al., 2014). Within permafrost landscapes, the mobility potential of nutrients is largely dependent on both the topographic gradient and active layer depth, which also influence soil redox conditions (O'Donnell and Jones, 2006) and vegetation (Ogawa et al., 2006).

40   Previous studies have determined that more research is needed to constrain $N_2$-fixing vegetation and topographic controls on $NO_3^-$ mobility in the Arctic (Whigham et al., 2017; Harms et al., 2019; Harms and Ludwig, 2016). Near-surface hydrologic and drainage conditions in permafrost Arctic landscapes are influenced by the seasonal thaw of shallow active layer soils (Romanovsky and Osterkamp, 2000; Yano et al., 2010; Boike et al., 2018). Deeper active layers can result in the growth and expansion of larger plant types (including shrubs) that require drier soils and deeper thaw to accommodate their root systems

45   (Myers-Smith et al., 2011). The phenomenon of shrubs increasing in density and abundance in permafrost landscapes, is known as 'shrub expansion' or 'shrubification' (Tape et al., 2006; Weintraub and Schimel, 2003; Frost and Epstein, 2014; Ju and Masek, 2016; Myers-Smith et al., 2015; Sturm et al., 2001).

Certain shrub genera are more closely associated with climate-induced shrubification than others. *Alnus viridis* spp. *fruticosa*

50   (Siberian alder), for example, is a shrub species (Myers-Smith et al., 2011) that fixes atmospheric nitrogen ($N_2$) through the symbiotic relationship with *Frankia* bacteria residing within nodules in the alder root systems (Roy et al., 2007). Alders frequently establish on steep hillslopes (Myers-Smith et al., 2011; Tape et al., 2012) and have been associated with elevated concentrations of $NO_3$-N in soil pore water in cold environments at high elevations like the Alps (Bühlmann et al., 2014; Hiltbrunner et al., 2014).

55

The effects of alder on soil chemistry and stream water chemistry have been investigated in alpine, subalpine, and upland systems (Hurd and Raynal, 2004; Bühlmann et al., 2014; Mitchell and Ruess, 2009; Shaftel et al., 2012; Whigham et al., 2017); however, very few of these studies have been conducted in Arctic permafrost landscapes. Rhoades et al. (2001) found that alders in permafrost soils of northwest Alaska influenced soil $NO_3$-N and measured high foliar N in various plant types growing

60   within alder understory, suggesting increased soil N below the shrubs. While the linkage between alders and soil N is clear, the variability of soil pore water $NO_3$-N in relation to alders, topography, redox conditions, and permafrost in the Arctic has not previously been studied in detail.

**1.2 Study objectives**

To study the influence of alder on soil chemistry in Arctic permafrost landscapes, we investigated the relationships that exist

65   between $N_2$-fixing alders, topography, and soil moisture to determine the dominant controls on $NO_3^-$ availability that occur in

permafrost soils situated in a hillslope landscape. We focused our research on a location where a recent study estimated that alder area coverage in the hillslope shrubland community increased by 40% from 7.4 ha in 1956 to 10.4 ha in 2014, with an average rate of alder expansion of 513 $m^2$ $yr^{-1}$ (Salmon et al., 2019a). Within this field setting, we hypothesize that: 1) $NO_3^-$ availability varies both spatially and temporally on short scales across permafrost landscapes; 2) proximity to alder shrublands is a dominant control on $NO_3^-$ availability in soil pore water and will be highest within and immediately downslope of alder stands; and 3) $NO_3^-$ mobility is limited by changes in redox conditions across the hillslope topographic gradient.

## 2 Materials and methods

### 2.1 Study location

Approximately 80 km north of the Alaskan coastal town of Nome and 12 km east of Mary's Igloo, the research hillslope of interest is located at mile marker 64 of Kougarok Road (65°09'50.1"N, 164 °49'34.2"W) and is referred to as the Kougarok Hillslope (KG Hillslope; Fig. 1). KG Hillslope is a prominent hillslope (elevation from 40-140 m.a.s.l.) with the Kuzitrin River to the north and west (~ 11° topographic slope) and a series of shallow thermokarst lakes to the east (~ 5° topographic slope). The site is composed of metagranitic Late Proterozoic bedrock outcropping at the top of the hill (Hopkins et al., 1955), and gives way to continuous permafrost on the lower slope which is likely Quaternary aged sediments composed of peat, alluvial sediment, and interlaced gravel lenses (Hopkins et al., 1955; Till et al., 2011). The hillslope is asymmetrical and slopes more steeply to the west than to the east (~ 11° and ~ 5° topographic slope, respectively). The KG Hillslope is overlain by an active soil layer containing organic peat and mineral horizons (taxonomic soil classification not available) and is well drained in the upland area due to topographic gradient.

Vegetation found in the upland area primarily includes alder growing in a densely populated alder shrubland community near the crest of the hill interspersed by lichen, moss, and dwarf shrubs. Vegetation in the lowland area is characterized by either alder savanna or tussock tundra plant communities (Iversen et al., 2016; Salmon et al., 2019b). The term 'alder savanna' was defined by Frost et al., (2013), who stated, 'Such shrubland communities, colloquially referred to as 'alder savannas', have been described at several locations in Low Arctic and interior montane Alaska (Racine 1976, Racine and Anderson 1979, Chapin et al., 1989). Regular spacing of alders in 'alder savannas' has been attributed to intra-specific competition for limiting nutrients (Chapin et al., 1989).'

Areas defined as *alder shrubland* communities are dominated by large stands that are exclusively alder and thrive on steep hillslopes (Tape et al., 2006, 2012; Salmon et al., 2019a-b). Whereas, *alder savannas* occur in weakly developed water tracks and consist of short alder dispersed with other deciduous shrub species and graminoids. Between the lowland alder savanna water tracks, tussock tundra plant communities lack alder and are characterized by graminoids (E.g. *Eriophorum vaginatum* and *Carex bigelowii*), dwarf shrubs (E.g. *Betula nana* ssp. *exilis*), lichens (E.g. *Cladonia* spp.) and moss (E.g. *Sphagnum* spp.).

A co-located study by Salmon et al. (2019a-b) defines the vegetation parameters of the hillslope in further detail including alder stand height, basal area and nodule biomass per shrub and per ground coverage. Active layer soils are deeper in the lowland area than the upland area soils, have a thicker organic peat horizon, and are poorly drained due to low topographic gradient (Salmon et al., 2019a-b). The lowland is frequently saturated in inter-tussock areas, especially at the slope break

105   between the steep upland area and shallow lowland area, and within the alder savanna community.

For our study, soil pore water compositions within alder shrubland in the upland area were compared to soil pore water compositions outside alder shrubland (both in upland and lowland areas; see Fig 1). These samples were collected over four field campaigns with a higher-resolution focus and additional monitoring at two alder patch transects (A1 and A4) during the

110   latter campaigns (Fig. 1; Fig. 2). The A1 transect includes a sampling location we identify as a 'seep', which is a direct seep from the ground located at the slope transition between upland and lowland zones (Fig. 1b). The volume of water sourced from this seep was too small to measure directly but is estimated to be $< 2$ cm$^3$ s$^{-1}$. However, water actively trickled from this seep location during all sampling campaigns and is likely representative of active layer melt that surfaced at the upland-lowland transition.

115   **2.2 Sample design**

To investigate the aforementioned hypotheses, this study was subdivided into two phases: an initial phase to identify $NO_3$-N 'hotspots' in relation to the alder shrubland community (Phase 1) and a comprehensive informed phase (Phase 2) to further address each of the three hypotheses. Phase 1 (July 18-21, 2017) consisted of a synoptic survey to establish soil $NO_3$-N variability within and adjacent to five upland alder shrubland areas (A1 – A5; Fig. 1a). To capture this variability, transects

120   were installed with sampling points located within alder shrubland as well as upslope and downslope of the shrubland. These transects also captured the transition between upland and lowland landscape position, which was determined to be located at the most downslope extent of each alder shrubland area.

Phase 2 (September 14-16, 2017, July 22-27, 2018 and September 21-22, 2018) sampling addressed the variability of $NO_3$-N

125   within and downslope of two of the alder shrubland areas (A1 and A4 transects; Fig. 1b) that were exposed to the same topographic and climatic conditions and examined this variability with respect to topographic gradient. The A1 and A4 transects are located at similar relief on the eastern slope near the crest of the KG Hillslope; however, the transects extend through and downslope of two separate alder patches allowing the nutrient dynamics associated with each shrubland area to be examined independently. These transects were examined with increasing resolution throughout sampling campaigns to

130   determine $NO_3$-N variability within the shrubland and to capture the extent of $NO_3^-$ availability down gradient of the shrubland (see Table S5 in the Supplemental material for further details of the number of sampling locations per transect for each campaign). To address these spatiotemporal controls, we measured soil pore water $NO_3$-N concentrations within, between, and downslope of alder shrubland, and measured the natural abundance of redox sensitive species (including manganese (Mn)

ferrous iron ($Fe^{2+}$), and sulfate ($SO_4^{2-}$)) along the transects to assess biogeochemical processes and controls on nutrient availability in soil pore water across the tundra. Although an important intermediate form of nitrogen, $NH_4^+$ was measured but is not discussed with detail in this study due to low dissolved concentrations in these pore water samples (Table S1; Supplemental material).

Soil pore water and bulk soil samples were collected from each sampling location to assess $NO_3$-N concentrations and any correlations with soil moisture. In Phase 1 (the July 2017 campaign), samples were collected at each of the five alder patches (Fig. 1a). In Phase 2, which spanned the three subsequent sampling campaigns, all samples were collected from the A1 and A4 transects (Fig. 1b), with the goal of examining spatial $NO_3$-N variations with higher resolution. The alder stand along the A1 transect covers roughly ~3,400 $m^2$ in area and is located 20 m north of the A4 transect, which intersects an alder stand covering roughly ~6,400 $m^2$ in area (Fig. 1b). Sample collection evolved from three sampling locations per transect in Phase 1 to sampling locations placed every 10 m along each transect in Phase 2, initiating within the alder shrubland and terminating 50 m downslope from the bottom of each shrubland area (Fig. 1b). The number of samples per location for each sampling campaign varied as spatial resolution increased through time and are shown in the associated Tables S4 and S5 in Supplemental material.

**2.3 Soil pore water**

Soil pore water samples are the basis of our $NO_3^-$-N availability and variability investigation and were collected by installing a nest of macro-rhizons at each sample location (Rhizosphere Research Products; hereafter referred to as rhizons) using the methods described by Seeberg-Elverfeldt et al., (2005). Rhizons were installed at depths between 15-30 cm, and due to the volume required for chemical analyses, were installed in nests (on average 5 rhizons per nest) at each sampling location depending on soil saturation and water availability. Soil pore water was collected in 60- ml syringes connected by luer-lock mechanisms on each rhizon. Syringes were subsequently combined into one sample per nest to obtain adequate volumes for analyses and ensure a homogenous bulk sample. Syringes were re-hung from rhizons at their respective sampling locations and left overnight before collection the next morning.

After the soil pore water collected from each nest was integrated for a representative sample, the samples were then filtered, frozen, and transported to Los Alamos National Laboratory's Geochemistry and Geomaterials Research Laboratory (GGRL) where they were stored frozen until undergoing geochemical analysis. Cations were measured using inductively coupled plasma optical emission spectrometry (ICP-OES) on a Perkin Elmer Optima 2100DV instrument (Perkin Elmer Inc., USA) using United States Environmental Protection Agency (EPA) method 200.7; precision is justified to 0.01 mg $L^{-1}$. Anions were measured with ion chromatography on a Dionex ICS-2100 instrument (Thermo Fisher Scientific Inc., USA) utilizing EPA method 300 (Throckmorton et al., 2015); precision is justified to 0.01 mg $L^{-1}$. Isotopic analyses including $\delta^{15}N$ and $\delta^{18}O$ of

soil pore water and soil pore water $NO_3$-N was also performed to gain insights to nitrate sources and likely biogeochemical

processes occurring in our study location (see associated Supplemental material for full details).

**2.4 Soil and leaf litter**

Soil and leaf litter samples were collected for comparison to soil pore water $NO_3$-N content and to assess possible correlations between parameters. Along the A1 and A4 transects, soil was collected for soil moisture analysis from 15-cm depths (and at 30-cm depths where soil was deep enough) in pre-weighed tins, sealed with parafilm, and frozen for preservation. Samples were not collected shallower than 15 cm depth because of the large presence of peat biomass at shallow depths and because all soil pore water samples were collected from ≥15 cm depths. A total of 27 soil samples were collected during July 2017, 6 during September 2017, and 24 in July 2018. It is worth noting that while our soil moisture and soil pore water samples were co-located, they were offset temporally with our soil moisture sampling occurring at the end of our campaigns to avoid perturbing the rhizon nests while we were actively collecting soil pore water samples.

 In July 2018, three soil pits (P1, P2, and P3) were dug and described along the A1 transect (Fig.1b). In each pit, soil was excavated to frozen soil, verified by presence of ice and sub-freezing soil temperatures. Soil was collected at an interval of 20 cm in each pit. Pits 3 and 1 had total depths of 46 cm and 55 cm to frozen soil, respectively, and soil samples were collected at 20 cm and 40 cm. Pit 2 had a depth of 61 cm to frozen soil and soil samples were collected at 20-, 40-, and 60-cm depths. All soil samples were frozen and transported to GGRL or North Carolina State University Department of Marine, Earth, and Atmospheric Sciences in Raleigh, North Carolina where they were stored frozen until analysis (See Supplemental material for additional details).

Alder leaf litter was collected in September 2018 from six locations along the A1 and A4 transects (3 samples from each transect), stored in sealed plastic bags, frozen, and homogenized prior to analysis (n=6). A contamination issue occurred with one of the leaf litter samples collected from the A4 transect, leaving us with n = 5. Thirteen soil samples and five leaf litter samples were analyzed for total N, $\delta^{15}N$ of soil organic nitrogen (SON) and C/N ratios (O'Donnell and Jones, 2006; Moatar et al., 2017; See Supplemental material for additional details).

**2.5 In situ parameters**

In-situ parameters were measured for each water sampling location to provide insights to environmental field conditions, including depth to frozen soil or bedrock, soil temperature at rhizon sampling depth (~15 cm), soil pore water pH, dissolved oxygen (DO), and specific conductivity. Summaries of DO, pH, and conductivity are provided in Table S2 (Supplemental material); no obvious spatial or temporal trends were observed within these parameters and no significant correlations with $NO_3$-N were observed ($r^2$ = 0.02, 0.2, 0.06, respectively). Iron (Fe) speciation parameters were collected for two days during

the July 2018 field campaign. These were mixed with ferrozine (to fix $Fe^{2+}$ for later analysis) on-site and subsequently analyzed at GGRL using the Fe-ferrozine method (Stookey, 1970). The Fe speciation method determined $Fe^{2+}$ and total Fe ($Fe_{Total}$; Stookey, 1970). $Fe^{3+}$ was later calculated as the difference between $Fe^{2+}$ and $Fe_{Total}$.

### 2.6 Statistical analyses

Data collected had normal distribution (identified through comparison of p-values to significance levels) and no outliers were identified. Thus, all measurements are included in the statistical analyses. Nonparametric Mann-Whitney rank sum tests were performed (Helsel and Hirsch, 2002) to identify significant differences between geochemical signatures - specifically $NO_3$-N, $Fe^{2+}$, $Fe_{Total}$, Mn, and $SO_4^{2-}$ - of soil pore water within the alder shrublands and outside the alder shrublands in Phases 1 and 2 (see Supplemental material). The Mann-Whitney statistical analyses performed quantified the spatial variability between upland (alder shrubland) and lowland (alder savanna) regions of our A1 and A4 transects collected during the July 2018 and September 2018 field campaigns and did not factor in temporal variability as our time-series were limited. The individual rhizon nests that composed the upland and lowland sampling sites are defined in Supplemental Table S5 and the detailed outcomes of the Mann-Whitney tests performed are provided in Supplemental Table S6. P-values less than 0.05 were considered statistically significant. Simple linear regressions were used to determine relationships between $NO_3$-N and variables including soil moisture, depth to frozen soil or bedrock, and Fe. MATLAB_R2017a was used for all statistical analyses and hydrochemical figure generation.

### 3 Results

#### 3.1 Soil depth and moisture

Soils within each upland patch were similar in composition with general defining characteristics of a surficial peat horizon underlain by decayed peat and a transitional horizon into mineral soil at a depth of ~12 to ~15 cm, followed by bedrock or frozen soil (personal observations of field participants; Salmon et al., 2019a-b). Soil composition, moisture, and active layer depth within the lowland portion of the A1 and A4 transects were similar but differed from the upland portion of the transects (Table S4; Supplemental material). During both Phase 1 and Phase 2, the mean gravimetric % soil moisture content ((weight of wet soil – weight of dry soil )/ weight of dry soil x 100) was lowest in the upland area (28.5%, 28.4%, and 36.6% in July 2017, September 2017, and July 2018 respectively) and greatest in the lowland area (>50%). The lowlands were inundated during the Phase 2 September 2017 campaign and contained standing water in various inter-tussock locations during the July 2017 and July 2018 sampling campaigns. The mean depth to bedrock or frozen soil was greater in the lowland area (mean of 56.5 cm and 54.3 cm in September 2017 and July 2018 respectively) than the upland area (mean of 45.7 cm and 36.6 cm in September 2017 and July 2018 respectively) during all but one sampling campaign (July 2017; Table S4; in Supplemental material). Soil moisture content and depth to bedrock or frozen soil were not measured during the September 2018 (September 21-22) sampling campaign due to logistical and sampling challenges.

### 3.2 Phase 1: initial results from five alder patches

From July 18-21 2017 soil pore water $NO_3^-$-N concentrations were significantly higher ($p < 0.01$) within the alder shrubland than sampling locations upslope and downslope of the shrubland along the A1, A2, A3, and A5 transects (Fig. 2a; additional details in Supplemental material). A precipitation event (with a high of ~13° C) occurred overnight on July 18th (Western Regional Climate Center, 2017) but unfortunately the field site rain gauge was out of commission and there is not a quantitative rain amount for this event. Parameters including soil depth, moisture content, pH, dissolved oxygen, and conductivity did not have apparent controls on $NO_3^-$-N and are reported in Tables S2 and S4 in Supplemental material. Soil pore water $NO_3^-$-N was initially negligible within the A1 alder shrubland (Fig. 3a) but increased in concentration following the rainfall event. A similar increase in $NO_3^-$-N was also observed at a seep located at the transition between the upland and lowland along the A1 transect on 19 July relative to the other sampling days from the initial July 2017 sampling campaign. This seep is likely representative of water flowing directly from within the A1 alder shrubland to the lowland area (Fig. 2b), perhaps through fractured bedrock. Phase 1 results show that soil pore water $NO_3^-$-N was elevated both from one alder shrubland patch to another (ranging from 0.3 mg L$^-$ to >10 mg L$^-$) and within alder shrubland relative to other sampling locations along each transect. The four-day sample collection along the A1 transect revealed daily variations in $NO_3^-$-N availability at our sampling locations (0.51 to 10.08 mg L$^{-1}$) likely associated with observed rainfall. Both the Road and the Middle transects located in the lowland tussock tundra and alder savanna communities had low $NO_3^-$-N (< 1.0 mg L$^{-1}$).

### 3.3 Phase 2: $NO_3^-$-N variability between two alder patches

#### 3.3.1 September 2017

During the 2017 September sampling campaign (September 14-18), conditions were cool (high of ~5.4° C), with daily precipitation (personal observation of field participants; Western Regional Climate Center, 2017). $NO_3^-$-N was elevated within the A4 shrubland and downslope of the A1 shrubland (Fig. 3b), but negligible in soil pore water collected from upland areas between the two transects. The mean $NO_3^-$-N concentration within the A1 and A4 transects did not vary significantly from the mean $NO_3^-$-N concentration directly downslope of the alder shrubland ($p > 0.05$; reference purple sampling locations in Fig. 1b). However, the mean concentration of $NO_3^-$-N both within and directly downslope of the shrublands was significantly greater ($p < 0.05$; Table S4 in Supplemental material) than the mean $NO_3^-$-N concentration of the Middle and Road transects in the furthest extent of the lowland area (Transects M and R in Fig. 1a), indicating that transport potential of $NO_3^-$-N is limited to near the slope break.

#### 3.3.2 July 2018

During the 2018 July sampling campaign (July 22-26th), $NO_3^-$-N was elevated along the A1 and A4 transects (Fig. 2b and Fig. 3c), both within the shrubland and up to 20-m downslope of the shrubland, where the transition between upland and lowland occurs (Fig. 3c). Each of the five sampling days in July were dry (no precipitation, high of ~16° C), and no notable temporal

variation (< 3 mg $L^{-1}$ difference) in $NO_3$-N was observed along the A1 and A4 transects (Fig. 4a-b). $NO_3$-N concentrations measured from two soil pits located along the A1 transect also increased with depth (Table S5, Supplemental material). Despite the dry conditions, we directly observed water seeping from the upslope wall into each pit, suggesting that interflow was actively occurring across the A1 transect from the upland to lowland areas. Nitrate-N concentrations decreased from upland to lowland along both the A1 and A4 transects (significantly different at $p < 0.001$; Table S5, S6 in Supplemental material). This pattern was mirrored by Fe, which increased in concentration from upland to lowland ($p < 0.001$) along each transect (Fig. 4b and Table S5, S6 in Supplemental material). Similarly, Mn increased from the upland to lowland along the A4 transect ($p < 0.05$; Fig. 4b and Table S5, S6 in Supplemental material). Spatial trends in Mn were not identified, however, along the A1 transect (Fig. 4a) with respect to Mn reduction ($p > 0.05$; Table S5, S6 in Supplemental material). No trends or significant difference ($p > 0.05$) in $SO_4^{2-}$ concentrations were observed along the A4 transect (Table S5, S6 in Supplemental material).

### 3.3.3 September 2018

In September 2018 ($21\text{-}22^{nd}$), similar patterns in $NO_3$-N concentration occurred along both A1 and A4 transects (Supplemental material), with the highest $NO_3$-N at locations within and directly downslope of the shrubland. Total Fe and $SO_4^{-2}$ did not vary along the A1 transect, but $Fe_{Total}$ increased along the A4 transect and $SO_4^{-2}$ increased between 0-20 m downslope of the alder shrubland (Table S5, Supplemental material). Manganese was negligible (< 0.01 mg $L^{-1}$) along both A1 and A4 transects. No precipitation events occurred during sampling in September 2018.

### 4 Discussion

### 4.1 Sources of nitrate

Previous studies conducted in continuous, polygonal permafrost areas without alders indicate that soil moisture is the dominant control on $NO_3^-$ production (Heikoop et al., 2015). However, at the KG Hillslope where polygonal permafrost features do not exist and the landscape is controlled by slope gradient rather than microtopography, no direct relationship was observed between and $NO_3$-N and soil moisture ($r^2 < 0.2$; Fig. S1 in Supplemental material). Instead of being associated with soil moisture, at this site, $NO_3$-N concentrations were tightly constrained by the presence of alder shrublands. Although $NO_3$-N was generally absent in the poorly drained (wet) lowland area, it was elevated within alder patches on the well-drained (dry) upland area. Elevated $NO_3$-N was not observed laterally adjacent to or upslope of alder shrubland. Therefore, while soil moisture likely plays a role in determining $NO_3$-N availability, our results indicate that the alder shrubland community was the dominant control on $NO_3$-N availability in soil pore water on the KG Hillslope. Furthermore, Darrouzet-Nardi and Weintraub (2014) found evidence for spatial inaccessibility of labile N in Arctic ecosystems due to isolation in environments with low water potential, but our findings indicate the potential for increased accessibility from the mobilization of labile N in the presence of topographic relief and precipitation. A detailed overview of the isotopic analyses performed and results are presented in the Supplemental online material, however, it is worth noting that the $\delta^{15}N$ and $\delta^{18}O$ of soil pore water were

consistent with the predicted range of $NO_3^-$ produced through microbial degradation of N-rich alder shrub organic matter. Enrichment of both $\delta^{15}N$ and $\delta^{18}O$ isotopes at wetter downslope locations indicate that denitrification limits the mobility of $NO_3^-$–N by transforming it to other N-species.

345

## 4.2 Effects of precipitation on pore water nitrate

Previous studies have linked nutrient flushing with rainfall events (Bechtold et al., 2003; Baldwin and Mitchell, 2000; Rasmussen et al., 2020; Rasmussen et al., 2022), and several studies have proposed that soil $NO_3^-$ inputs from mineralized and nitrified leaf litter are mobilized at wet-season onset (Yamashita et al., 2010; Bernal et al., 2003). In particular, Vink et al.,

350    (2007) found that in a forested catchment, inorganic N accumulated within soil and leaf litter during dry periods and was subsequently flushed into headwater streams during precipitation events – an initial pulse in $NO_3$-N in soil pore water quickly declined following increased precipitation and discharge. The dynamic short-term temporal variability of $NO_3$-N observed along the A1 transect (Fig 3; within and downslope of shrubland) that co-occurred with precipitation events in July and September of 2017 provides evidence that a similar model of $NO_3^-$ accumulation and subsequent mobilization occurs on the

355    KG Hillslope. A 'pulse-like' signal of elevated soil pore water $NO_3$-N was observed within and downslope of shrubland along the A1 transect (Fig. 3a) that occurred following an overnight precipitation event between July 17 – 18, 2017.

Rainfall occurred during sampling on all three days of the September 2017 campaign (9/14/17 through 9/16/17; personal observation; Western Regional Climate Center, 2017). During July 2018 (July 22-27) and September 2018 (September 21-22)

360    campaigns, weather conditions were much drier (no recorded precipitation events) and $NO_3$-N concentrations showed little variation with no daily pattern, ranging from 4.09 mg $L^{-1}$ to 4.94 mg $L^{-1}$ downslope of shrubland along the A1 transect over the five days in July 2018 and from 0.02 mg $L^{-1}$ to 0.12 mg $L^{-1}$ over two days in September 2018. While the precipitation events in July 2017 and September 2017 likely mobilized $NO_3^-$ from the shrubland to the lowland area (down gradient) along the A1 transect, this mobility was only observed within the first 10-30 m downslope of the shrubland (Fig. 4a), indicating the

365    presence of additional controls (such as denitrification bacteria, assimilation, and hydrologic flushing) acting on $NO_3^-$ transport across the landscape.

## 4.3 Effects of redox on pore water nitrate-N

The decrease in soil pore water $NO_3$-N along the A1 and A4 transects and increase in soil moisture, $Fe^{2+}$, and Mn along the

370    A4 transect in July 2018 (Fig. 4) and September 2018 (Tables S5, S6, in Supplemental material) indicate a transition from an oxic environment towards a more sub-oxic environment as the slope transitions from upland to lowland. The lack of variation in $SO_4^{-2}$ across these transects indicates that conditions were not reducing enough for sulfate reduction or methanogenesis (Jakobsen and Postma, 1999). Our data indicate that the oxic environment on the well-drained upland slope supports $NO_3$-N

Deleted: ⁻

Deleted: ⁻

Deleted: associated

Deleted: ⁻

Deleted: corresponded to a

Deleted: which occurred overnight

Deleted: This event is reflected in the $\delta^{18}O$ - $NO_3^-$ of two samples collected within shrubland along the A1 transect during this time period, where enriched values of $\delta^{18}O$ (> 10.0 ‰; Fig. S2 in Supplemental material) may indicate a minor influence by atmospheric deposition of $NO_3^-$.

Deleted: ⁻

Deleted: did appear to

Deleted: ⁻

Deleted: ⁻

production while sub-oxic environment of the poorly drained lowland area supports the reduction or denitrification of $NO_3^-$

390 (Table S5 in Supplemental material).

Callahan et al., (2017) described upland hillslope alders as 'hotspots' for $NO_3^-$ inputs into streams at the hillslope scale, and Harms and Jones (2012) observed greater $NO_3^-$ export in soils with increased active layer thickness. These predictions are consistent with the elevated $NO_3$-N concentrations within and directly downslope of alder shrubland along each transect (Fig.

395 4). The prevailing sub-oxic conditions downslope of A1 and A4 and overall scarcity of inorganic N likely restrict $NO_3^-$ production, indicating that elevated $NO_3$-N concentrations observed at these locations was produced within the alder shrubland patches and flushed downslope. However, mobility of $NO_3^-$ beyond the first 20-30 m downslope of shrubland along the A1 and A4 transects was not observed (Fig. 4). Inputs and subsequent dilution from flow along the gradient may be responsible for the decrease in $NO_3$-N, but it is more likely due to denitrification occurring in the sub-oxic conditions, as evidenced by the

400 isotopic denitrification trend observed (see Supplemental material for full isotopic discussion). Consistent with these results, a study by Harms and Ludwig (2016) predicted that saturated soils and reducing conditions may buffer N export to downslope ecosystems. Thus, while hillslopes dominated by alder will likely increase $NO_3^-$ availability with shrubification, sub-oxic to reducing zones and soil saturation occurring at downslope locations may serve as buffers to down gradient mobility of $NO_3^-$ through microbial denitrification. Defining the role of topographically controlled redox environments on nutrient cycling in

405 permafrost environments will be beneficial for understanding the likelihood of $NO_3^-$ mobilization to streams and subsequent transport down-gradient within N-limited landscapes.

### 4.4 Spatial and temporal variations in nitrate-N

Over the limited time series we collected in the 2017 and 2018 growing seasons, significant ($p < 0.05$; Supplemental material) spatiotemporal variability of soil pore water $NO_3$-N concentrations were observed at our continuous permafrost site with a

410 distinct ridge-toe slope topography. Spatial variability existed within individual shrubland areas as well as from one shrubland area to another (Fig. 2; Table S5 in Supplemental material). These spatial differences encompassed both changes in the distribution of $NO_3$-N within alder shrubland and changes in the magnitude of $NO_3$-N present in the landscape over time. Temporally, we observed dynamic daily variability in $NO_3$-N that co-occurred with precipitation events at locations within and downslope of two alder shrubland patches (Fig. 3).

415

Although soil pore water $NO_3$-N was elevated during dry conditions and active drainage through-flow was observed in open soil pits, the notable day-to-day changes in $NO_3$-N during wet conditions indicate that this variability was likely influenced by the co-occurrence of rainfall as a mobilization mechanism. Evidence for this mechanism was observed during or following precipitation events; first after the isolated precipitation event in July 2017 where $NO_3$-N concentrations were elevated both

420 within and downslope of alder shrubland in one location (Fig. 3a), and again in September 2017 where $NO_3$-N concentrations were elevated downslope but not within the same shrubland (Fig. 3b). On the KG Hillslope, $NO_3^-$ likely accumulates in the

soil below alders as litter decomposes (supported by isotopic evidence presented in Supplemental material) and is likely mobilized down-gradient with the onset of rainfall. These spatial variations that co-occur with rainfall events likely indicate a 'flushing' down gradient of previously accumulated soil $NO_3^-$ from within the alder shrubland, and highlight the capacity for $NO_3^-$ to be mobilized across landscapes.

**4.5 Future research**

Findings from this study illuminate a level of complexity in N cycling that is not widely published by providing snapshots of variability and mobility of $NO_3^-$ on the KG Hillslope over brief time series. Future studies would benefit from the additional incorporation of continuous monitoring of $NO_3^-$ throughout a growing season (starting around snowmelt; Rasmussen et al., 2022), consideration of alder characteristics (biomass, root and nodule density, rates of N fixation; Salmon et al., 2019a-b), and targeted transects throughout a permafrost alder landscape (as done in this study) to further characterize spatial variation in soil pore water $NO_3^-$ in relation to alder stand proximity. Studies to further identify processes controlling the availability, transport, and fate of N in permafrost landscapes would benefit from the inclusion of N sources, total N input, organic carbon, microbial community function, and C:N relationships, such as those conducted by Ramm et al. (2020). Long-term impacts of $NO_3^-$ on vegetation, permafrost degradation, and interstitial water chemistry in wet downslope permafrost landscapes also require further investigation. Moreover, identification of microbial communities in the sub-oxic reducing downslope environments would lend insights towards the fate of $NO_3^-$, whether it is assimilated by plants or reduced to $N_2$ or nitrous oxide gas.

Furthermore, the dynamic variability of $NO_3$-N across the KG Hillslope indicates the importance of improving the representation of N cycle processes in ESMs. Although plant functional types (PFTs) are included in ESMs currently, processes such as N-fixation remain underrepresented in these classifications (Wullschleger et al., 2014), and their incorporation to ESMs could improve nutrient availability and variability predictions.

**5 Conclusion**

Teasing apart the dynamics between alder shrubland communities, topography, permafrost, and $NO_3^-$ availability is complex because interactions between these factors vary both across time and space. The high degree of $NO_3$-N variability observed over short timescales (days) and distances (meters) is documented in this study. The existence of a topographic gradient within our alder shrubland landscape allows for precipitation events to mobilize nitrate downslope. However, redox environments driven by hillslope topography are important factors in limiting the spatial extent of $NO_3^-$ mobility across permafrost landscapes. These findings have implications for the anticipated nutrient responses associated with the expansion of shrub vegetation in the Arctic and demonstrate the importance of incorporating factors such as topography, redox conditions, and plant functional type in watershed scale studies. Along with permafrost thaw (Harms and Jones, 2012) and changes in soil moisture distribution (Heikoop et al., 2015), the expansion of $N_2$-fixing shrubs across tundra landscapes is a dominant

475 mechanism that could greatly increase local $NO_3^-$ availability in the Arctic. However, this study demonstrates that to fully account for the impact of shrubification on $NO_3^-$ availability and export, scientists should also consider topographic gradients, hydrologic conditions, and the presence of geochemical reducing zones that may affect $NO_3^-$ fate and transport.

*Data Availability.* The complete data set for this research can be accessed at https://doi.org/10.5440/1544760.

*Author Contributions.* REM, CAA, BDN, JMH, VGS, and CJW conceptualized the study. REM, CAA, BDN, JMH, VGS, SS,
480 and NAW contributed to the study investigation. REM, CAA, BDN, VGS, and JMH performed formal analyses of the data. REM, CAA, BDN, JMH, GBP, and OCM contributed to data curation of this project. CJW and SDW were involved in funding acquisition, project administration, supervision, and resource access. JMH, GBP and OCM provided laboratory resources for this project. REM, CAA, BDN, VGS, and JMH were involved in visualization, the writing of the original draft preparation and the review and editing process. CJW, SS, NAW, and SDW contributed to writing review and editing.

485 *Competing Interests.* The authors declare they have no conflicts of interest.

*Acknowledgements.* This research was completed with oversight and support of the Next-Generation Ecosystems Experiments (NGEE Arctic) project. NGEE Arctic is supported by the Office of Biological and Environmental Research in the U.S. Department of Energy – Office of Science. Support for this research was also provided by the Earth and Environmental Sciences Division at Los Alamos National Laboratory (LANL), the Geological Society of America, and the Marine, Earth,
490 and Atmospheric Sciences (MEAS) Department at North Carolina State University. We would like to thank Mary's Igloo Native Corporation for their guidance and for allowing us to conduct this research on the traditional homelands of the Iñupiat people. We would like to thank Nate Conroy, Emma Lathrop, Emily Kluk, Dea Musa, and the staff at the Geochemistry and Geomaterials Research Laboratory at LANL for their assistance in fieldwork, laboratory analysis, and data organization. We thank Bob Busey for access to continuous weather data. Thank you to the entire NGEE Arctic team for their support. Finally,
495 we would like to thank Ethan Hyland and Gwen Hopper for laboratory assistance in the MEAS Department at North Carolina State University.

**References**

Baldwin, D. S., and Mitchell, A. M.: The effects of drying and re-flooding on the sediment and soil nutrient dynamics of lowland river-floodplain systems: A synthesis, Regul. Rivers: Res. Mgmt., 16, 457–467, https://doi.org/10.1002/1099-
500 1646(200009/10)16:5<457::AID-RRR597>3.3.CO;2-B, 2000.

Barnes, R. T., Williams, M. W., Parman, J. N., Hill, K., and Caine, N.: Thawing glacial and permafrost features contribute to nitrogen export from Green Lakes Valley, Colorado Front Range, USA, Biogeochemistry, 117, 413–430, https://doi.org/10.1007/s10533-013-9886-5, 2014.

Bechtold, J. S., Edwards, R. T., and Naiman R. J.: Biotic versus hydrologic control over seasonal nitrate leaching in a floodplain forest, Biogeochemistry, 63, 53–72, https://doi.org/10.1023/A:1023350127042, 2003.

Bernal, S., Butturini, A., Nin, E., Sabater, F., and Sabater, S.: Leaf litter dynamics and nitrous oxide emission in a Mediterranean riparian forest, J. Environ. Qual., 32, 191–197, https://doi.org/10.2134/jeq2003.1910, 2003.

Boike, J., Juszak, I., Lange, S., Chadburn, S., Burke, E., Overduin, P. P., and Westermann S.: A 20-year record (1998–2017) of permafrost, active layer and meteorological conditions at a high Arctic permafrost research site (Bayelva, Spitsbergen), Earth Syst. Sci. Data, 10, 355–390, https://doi.org/10.5194/essd-10-355-2018, 2018.

Bühlmann, T., Hiltbrunner, E., and Körner, C.: *Alnus viridis* expansion contributes to excess reactive nitrogen release, reduces biodiversity and constrains forest succession in the Alps, Alp. Bot., 124, 187–191, https://doi.org/10.1007/s00035-014-0134-y, 2014.

Callahan, M. K., Whigham, D. F., Rain, M. C., Rains, K. C., King, R. S., Walker, C. M., Maurer, J. R., and Baird, D. J.: Nitrogen subsidies from hillslope alder stands to streamside wetlands and headwater streams, Kenai Peninsula, Alaska, JAWRA, 53, 478–492, https://doi.org/10.1111/1752-1688.12508, 2017.

Chapin, F. S., McGraw, J. B., and Shaver, G. R. Competition causes regular spacing of alder in Alaskan shrub tundra. Oecologia 79, 412–416, https://doi.org/10.1007/BF00384322, 1989.

Chapin, F. S., Mcguire, A., D., Randerson, J., Pielke, R., Baldocchi, D., Hobbie, S. E., Roulet, N., Eugster, W., Kasischke, E., Rastetter, E. B., Zimov, A., and Running, S. W.: Arctic and boreal ecosystems of western North America as components of the climate system, Glob. Chang. Biol., 6, 211–223, https://doi.org/10.1046/j.1365-2486.2000.06022.x, 2000.

Darrouzet-Nardi, A., and Weintraub, M. N.: Evidence for spatially inaccessible labile N from a comparison of soil core extractions and soil pore water lysimetry, Soil Biol. Biochem., 73, 22–32, https://doi.org/10.1016/j.soilbio.2014.02.010, 2014.

Frost, G. V., Epstein, H. E., Walker, D. A., Matyshak, G., and Ermokhina, K. Patterned-ground facilitates shrub expansion in Low Arctic tundra. Environ. Res. Lett. 8, 015035. https://doi.org/10.1088/1748-9326/8/1/015035, 2013.

Frost, G. V., and Epstein, H. E.: Tall shrub and tree expansion in Siberian tundra ecotones since the 1960s, Glob. Chang. Biol., 20, 1264–1277, https://doi.org/10.1111/gcb.12406, 2014.

Harms, T. K., and Jones, J. B.: Thaw depth determines reaction and transport of inorganic nitrogen in valley bottom permafrost soils, Glob. Chang. Biol., 18, 2958–2968, https://doi.org/10.1111/j.1365-2486.2012.02731.x, 2012.

Harms, T. K., and Ludwig, S. M.: Retention and removal of nitrogen and phosphorus in saturated soils of Arctic hillslopes,
535    Biogeochemistry, 127, 291–304, https://doi.org/10.1007/s10533-016-0181-0, 2016.

Harms, T. K., Cook, C. L., Wlostowski, A. N., Gooseff, M. N., and Godsey, S.E.: Spiraling down hillslopes: nutrient uptake
from water tracks in a warming Arctic, Ecosystems, 22, 1546–60, https://doi.org/10.1007/s10021-019-00355-z, 2019.

Heikoop, J. M., Throckmorton, H. M., Newman, B. D., Perkins, G. B., Iversen, C. M., Chowdhury, T. R., Romanovsky, V.,
Graham, D. E., Norby, R. J., Wilson, C. J., and Wullschleger, S. D.: Isotopic identification of soil and permafrost nitrate
540    sources in an Arctic tundra ecosystem, J. Geophys. Res. Biogeosci., 120, 1000– 1017, https://doi:10.1002/2014JG002883,
2015.

Helsel, D. R., and Hirsch, R. M.: Statistical methods in water resources: Techniques of water resources investigations, 04-A3,
U.S. Geological Survey, Reston, VA, USA, 118-122, https://doi:10.3133/twri04A3, 2002.

Hiltbrunner, E., Aerts, R., Bühlmann, T., Huss-Danell, K., Magnusson, B., Myrold, D. D., Reed, S. C., Sigurdsson, B. D., and
545    Körner, C.: Ecological consequences of the expansion of N2-fixing plants in cold biomes, Oecologia, 176, 11–24,
https://doi.org/10.1007/s00442-014-2991-x, 2014.

Hinzman, L. D., Deal, C. J., McGuire, A. D., Mernild, S. H., Polyakov, I. V., and Walsh, J. E.: Trajectory of the Arctic as an
integrated system, Ecol. Appl., 23, 1837–1868, https://doi.org/10.1890/11-1498.1, 2013.

Hopkins, D. M., Karlstrom, T. N. V.: Permafrost and groundwater in Alaska, 264-F, US Government Printing Office, United
550    States, Washington D. C., 122-124, 1955.

Hovelsrud, G. K., Poppel, B., van Oort, B., and Reist, J. D.: Arctic societies, cultures, and peoples in a changing cryosphere,
AMBIO, 40, 100–110, https://doi.org/10.1007/s13280-011-0219-4, 2011.

Hurd, T. M., and Raynal, D. J.: Comparison of nitrogen solute concentrations within alder (Alnus incana ssp. rugosa) and non-
alder dominated wetlands, Hydrol. Process., 18, 2681–2697, https://doi.org/10.1002/hyp.5575, 2004.

555    Iversen, C., Breen, A., Salmon, V., Vander Stel, H., and Wullschleger, S. D.: NGEE Arctic Plant Traits: Vegetation plot
locations, ecotypes, and photos, Kougarok Road mile marker 64, Seward Peninsula, Alaska, 2016, Next Generation Ecosystem
Experiments Arctic [data set], https://doi:10.5440/1346196, 2016.

Jakobsen, R. and Postma, D.: Redox zoning, rates of sulfate reduction and interactions with Fe-reduction and methanogenesis
in a shallow sandy aquifer, Rømø, Denmark, Geochim. Cosmochim. Acta, 63, 137-151, https://doi.org/10.1016/S0016-
560    7037(98)00272-5, 1999.

Ju, J., and Masek, J. G.: The vegetation greenness trend in Canada and US Alaska from 1984–2012 Landsat data, Remote Sens. Environ., 176, 1-16, https://doi.org/10.1016/j.rse.2016.01.001, 2016.

Keuper, F., Dorrepaal, E., van Bodegom, P. M., van Logtestijn, R., Venhuizen, G., van Hal, J., and Aerts, R.: Experimentally increased nutrient availability at the permafrost thaw front selectively enhances biomass production of deep-rooting subarctic peatland species, Glob. Change Biol., 23, 4257–4266, https://doi.org/10.1111/gcb.13804, 2017.

Koch, J. C., Runkel, R. L., Striegl, R., and McKnight, D. M.: Hydrologic controls on the transport and cycling of carbon and nitrogen in a boreal catchment underlain by continuous permafrost, J. Geophys. Res.: Biogeosci., 118, 698–712, https://doi.org/10.1002/jgrg.20058, 2013.

Martin, P. D., Jenkins, J. L., Adams, F. J., Torre, M., Matz, A. C., Payer, D. C., Reynolds, P. E., Tidwell, A. C., and Zelenak, J. R.: Wildlife response to environmental Arctic change: Predicting Future Habitats of Arctic Alaska, report from: The Wildlife Response to Environmental Arctic Change (WildREACH): Predicting future habitats of Arctic Alaska workshop, Fairbanks, AK, USA, 17-18 November 2008.

McClelland, J. W., Stieglitz, M., Pan, F., Holmes, R. M., and Peterson, B. J.: Recent changes in nitrate and dissolved organic carbon export from the upper Kuparuk River, North Slope, Alaska: N and C export from the Kuparuk River, J. Geophys. Res.: Biogeosci., 112, G4, https://doi.org/10.1029/2006JG000371, 2007.

Mitchell, J. S., and Ruess, R. W.: N2 fixing alder (*Alnus viridis* spp. *fruticosa*) effects on soil properties across a secondary successional chronosequence in interior Alaska, Biogeochemistry, 95, 215–229, https://doi.org/10.1007/s10533-009-9332-x, 2009.

Moatar, F., Abbot, B. W., Minaudo, C., Curie, F., Pinay, G.: Elemental properties, hydrology, and biology interact to shape concentration-discharge curves for carbon, nutrients, sediment, and major ions. Water Resour. Res., 53: 1270-1287, https://doi.org/10.1002/2016WR019635, 2017.

Myers-Smith, I. H., Forbes, B. C., Wilmking, M., Hallinger, M., Lantz, T., Blok, D., Tape, K. D., Macias-Fauria, M., Sass-Klaassen, U., and Lévesque, E.: Shrub expansion in tundra ecosystems: dynamics, impacts and research priorities, Environ. Res. Lett., 6, 045509, https://doi.org/10.1088/1748-9326/6/4/045509, 2011.

Myers-Smith, I. H., Elmendorf, S. C., Beck, P. S. A., Wilmking, M., Hallinger, M., Blok, D, Tape, K. D., Rayback, S. A., Macias-Fauria, M., Forbes, B. C., Speed, J. D. M., Boulanger-Lapointe, N., Rixen, C., Lévesque, E., Schmidt, N. M., Baittinger, C., Trant, A. J., Hermanutz, L., Collier, L. S., Dawes, M. A., Lantz, T. C., Weijers, S., Jørgensen, R. H., Buchwal, A., Buras, A., Naito, A. T., Ravolainen, V., Schaepman-Strub, G., Wheeler, J. A., Wipf, S., Guay, K. C., Hik, D. S., and

Vellend, M.: Climate sensitivity of shrub growth across the tundra biome, Nat. Clim. Chang., 5, 887–891, https://doi.org/10.1038/nclimate2697, 2015.

O'Donnell, J. A., and Jones, J. B.: Nitrogen retention in the riparian zone of catchments underlain by discontinuous permafrost, Freshw. Biol., 51, 854–864, https://doi.org/10.1111/j.1365-2427.2006.01535.x, 2006.

Ogawa, A., Shibata, H., Suzuki, K., Mitchell, M. J., and Ikegami, Y.: Relationship of topography to surface water chemistry with particular focus on nitrogen and organic carbon solutes within a forested watershed in Hokkaido, Japan, Hydrol. Process., 20, 251–265, https://doi.org/10.1002/hyp.5901, 2006.

Racine, C. H. Flora and vegetation: Biological Survey of the Proposed Kobuk Valley National Monument. Final Report ed H. R. Melchior (Fairbanks, AK: Alaska Cooperative Park Studies Unit, Biology and Resource Management Program, University of Alaska) pp 39–139, 1976.

Racine, C. H. and Anderson, J. H. Flora and vegetation of the Chukchi-Imuruk area Biological Survey of the Bering Land Bridge National Monument: Revised Final Report ed H. R. Melchior (Fairbanks, AK: Alaska Cooperative Park Studies Unit, Biology and Resources Management Program, University of Alaska) pp 38–113, 1979.

Ramm, E., Liu, C., Wang, X., Yue, H., Zhang, W., Pan, Y., Schloter, M., Gschwendtner, S., Mueller, C. W., Hu, B., Rennenberg, H., and Dannenmann, M.: The forgotten nutrient - The role of nitrogen in permafrost soils of Northern China, Adv. Atmos. Sci., 37, 793-799, https://doi.org/10.1007/s00376-020-0027-5, 2020.

Rasmussen, L. H., Ambus, P., Jansson, P.-E., Michelsen, A., and Elberling, B.: Slope hydrology and permafrost: The effect of snowmelt N transport on downslope ecosystem, Geophys. Res. Abstr., 22, https://doi.org/10.5194/egusphere-egu2020-2927, 2020.

Rasmussen, L. H., Zhang, W., Ambus, P., Michelsen, A., Jansson, P.-E., Kitzler, B., and Elberling, B.: Nitrogen transport in a tundra landscape: the effects of early and late growing season lateral N inputs on arctic soil and plant N pools and N2O fluxes, Biogeochem., 157, 69-84, https://doi.org/10.1007/s10533-021-00855-y, 2022.

Rhoades, C., Óskarsson, H., Binkley, D., and Stottlemyer, R.: Alder (Alnus crispa) effects on soils in ecosystems of the Agashashok River valley, northwest Alaska, Ecoscience, 8, 89-95, https://doi.10.1080/11956860.2001.11682634, 2001.

Romanovsky, V. E., and Osterkamp, T. E.: Effects of unfrozen water on heat and mass transport processes in the active layer and permafrost, Permafrost Periglac., 11, 219–239. https://doi.org/10.1002/1099-1530(200007/09)11:3<219::AID-PPP352>3.0.CO;2-7, 2000.

Roy, S., Khasa, D. P., and Greer, C. W.: Combining alders, frankiae, and mycorrhizae for the revegetation and remediation of contaminated ecosystems, Can. J. Bot., 85, 237–251, https://doi.org/10.1139/B07-017, 2007.

Salmon, V. G., Soucy, P., Mauritz, M., Celis, G., Natali, S. M., Mack, M. C., and Schuur, E. A. G.: Nitrogen availability increases in a tundra ecosystem during five years of experimental permafrost thaw, Glob. Chang. Biol., 22, 1927-1941, https://doi:10.1111/gcb.13204, 2016.

Salmon, V. G., Breen, A. L., Kumar, J., Lara, M. J., Thornton, P. E., Wullschleger ,S. D., and Iversen, C. M.: Alder distribution and expansion across a tundra hillslope: Implications for local N cycling, Front. Plant Sci., 10:1099. https://doi:10.3389/fpls.2019.01099, 2019a.

Salmon, V. G., Iversen, C. M., Breen, A. L., Vander Stel, H., and Childs, J.: NGEE Arctic Plant Traits: Plant Biomass and Traits, Kougarok Road Mile Marker 64, Seward Peninsula, Alaska, beginning 2016, Next Generation Ecosystem Experiments Arctic [data set], https://doi.org/10.5440/1346199, 2019b.

Schuur, E. A. G., McGuire, A. D., Schädel, C., Grosse, G., Harden, J. W., Hayes, D. J., Hugelius, G., Koven, C. D., Kuhry, P., Lawrence, D. M., Natali, S. M., Olefeldt, D., Romanovsky, V. E., Schaefer, K., Turetsky, M. R., Treat, C. C., and Vonk, J. E.: Climate change and the permafrost carbon feedback, Nature, 520, 171–179, https://doi.org/10.1038/nature14338, 2015.

Seeberg-Elverfeldt, J., Schlüter, M., Feseker, T., and Kölling, M.: Rhizon sampling of porewaters near the sediment-water interface of aquatic systems, Limn. Oceanogr. Methods, 3, 361–371, https://doi.org/10.4319/lom.2005.3.361, 2005.

Shaftel, R. S., King, R. S., and Back, J. A.: Alder cover drives nitrogen availability in Kenai lowland headwater streams, Alaska, Biogeochemistry, 107, 135–148, https://doi.org/10.1007/s10533-010-9541-3, 2012.

Sharkhuu, N., and Sharkhuu, A.: Effects of climate warming and vegetation cover on permafrost of Mongolia, in: Eurasian Steppes. Ecological Problems and Livelihoods in a Changing World, edited by: Werger, M. J. A., and van Staalduinen, M. A., Springer Netherlands, Heidelberg, Germany, 445–472, https://doi.org/10.1007/978-94-007-3886-7_17, 2012.

Shaver, G. R., and Chapin, F. S.: Response to fertilization by various plant growth forms in an Alaskan tundra: Nutrient accumulation and growth, Ecology, 61, 662–675, https://doi.org/10.2307/1937432, 1980.

Stookey, L. L.: Ferrozine-A new pectrophotometric reagent for iron, Anal. Chem., 42, 779-781, https://doi: 10.1021/ac60289a016, 1970.

Street, L. E., Burns, N. R., and Woodin, S. J.: Slow recovery of High Arctic heath communities from nitrogen enrichment, New Phytol., 206, 682–695, https://doi.org/10.1111/nph.13265, 2015.

Sturm M., Racine, C., and Tape, K.: Increasing shrub abundance in the Arctic, Nature, 411, 546–547, https://doi.org/10.1038/35079180, 2001.

645 Sulman, B. N., Salmon, V. G., Iversen, C. M., Breen, A. L., Yuan, F., and Thornton, P. E. Integrating Arctic plant functional types in a land surface model using above- and belowground field observations. J. Adv. Model. 13, e2020MS002396, https://doi.org/10.1029/2020MS002396, 2021.

Tape, K. D., Sturm, M., and Racine, C.: The evidence for shrub expansion in Northern Alaska and the Pan-Arctic, Glob. Chang. Biol., 12, 686–702, https://doi.org/10.1111/j.1365-2486.2006.01128.x, 2006.

650 Tape, K. D., Hallinger, M., Welker, J. M., and Ruess, R. W.: Landscape heterogeneity of shrub expansion in Arctic Alaska, Ecosystems, 15, 711–724, https://doi.org/10.1007/s10021-012-9540-4, 2012.

Throckmorton, H. M., Heikoop, J. M., Newman, B. D., Altmann, G. L., Conrad, M. S., Muss, J. D., Perkins, G. B., Smith, L. J., Torn, M. S., Wullschleger, S. D., and Wilson, C. J.: Pathways and transformations of dissolved methane and dissolved inorganic carbon in Arctic tundra watersheds: Evidence from analysis of stable isotopes, Global Biogeochem. Cycles, 29, 655 1893–1910, https://doi:10.1002/2014GB005044, 2015.

Till, A. B., Dumoulin, J. A., Werdon, M. B., and Bleick, H. A.: Bedrock geologic map of the Seward Peninsula, Alaska, and accompanying conodont data, USGS Scientific Investigations Map 3131, 75 pp., 2011.

Vink, S., Ford, P. W., Bormans M., Kelly, C., and Turley, C.: Contrasting nutrient exports from a forested and an agricultural catchment in south-eastern Australia, Biogeochemistry, 84, 247–264, https://doi.org/10.1007/s10533-007-9113-3, 2007.

660 Vitousek, P. M., Aber, J. D., Howarth, R. W., Likens, G. E., Matson, P. A., Schindler, D. W., Schlesinger, W. H., and Tilman, D. G.: Human alteration of the global nitrogen cycle: Sources and consequences, Ecol. Appl., 7, 737–750, https://doi.org/10.1890/1051-0761(1997)007[0737:HAOTGN]2.0.CO;2, 1997.

Walvoord, M. A., and Kurylyk, B. L.: Hydrologic impacts of thawing permafrost - A review, Vadose Zone J., 15, 1-20, https://doi:10.2136/vzj2016.01.0010, 2016.

665 Weintraub, M. N., and Schimel, J. P.: Interactions between carbon and nitrogen mineralization and soil organic matter chemistry in Arctic tundra soils, Ecosystems, 6, 129–143, https://doi.org/10.1007/s10021-002-0124-6, 2003.

Weintraub, M. N., and Schimel, J. P.: Nitrogen cycling and the spread of shrubs control changes in the carbon balance of Arctic tundra ecosystems, BioScience, 55, 408–415, https://doi.org/10.1641/0006-3568(2005)055[0408:NCATSO]2.0.CO;2, 2005.

670 Western Regional Climate Center: RAWS USA Climate Archive, retrieved from: https://raws.dri.edu/cgi-bin/rawMAIN.pl?akAQTZ, 2017.

Whigham, D. F., Walker, C. M., Maurer, J., King, R. S., Hauser, W., Baird, S., Keuskamp, J. A., and Neale, P. J.: Watershed influences on the structure and function of riparian wetlands associated with headwater streams - Kenai Peninsula, Alaska, Sci. Total Environ., 599, 124–134, https://doi.org/10.1016/j.scitotenv.2017.03.290, 2017.

675 Wullschleger, S. D., Epstein, H. E., Box, E. O., Euskirchen, E. S., Goswami, S., Iversen, C. M., Kattge, J., Norby, R. J., van Bodegom, P. M., and Xu, Z.: Plant functional types in Earth system models: past experiences and future directions for application of dynamic vegetation models in high-latitude ecosystems, Ann. Bot., 114, 1–16, https://doi.org/10.1093/aob/mcu077, 2014.

Yamashita, N., Ohta, S., Sase, H., Luangjame, J., Visaratana, T., Kievuttinon, B., and Kanzaki, M.: Seasonal and spatial
680 variation of nitrogen dynamics in the litter and surface soil layers on a tropical dry evergreen forest slope, For. Ecol. Manage., 259, 1502–1512, https://doi.org/10.1016/j.foreco.2010.01.026, 2010.

Yano, Y., Shaver, G. R., Giblin, A. E., Rastetter, E. B., and Nadelhoffer, K. J.: Nitrogen dynamics in a small Arctic watershed: retention and downhill movement of 15N, Ecol. Monogr., 80, 331-351, https://doi:10.1890/08-0773.1, 2010.

685 **Figures**
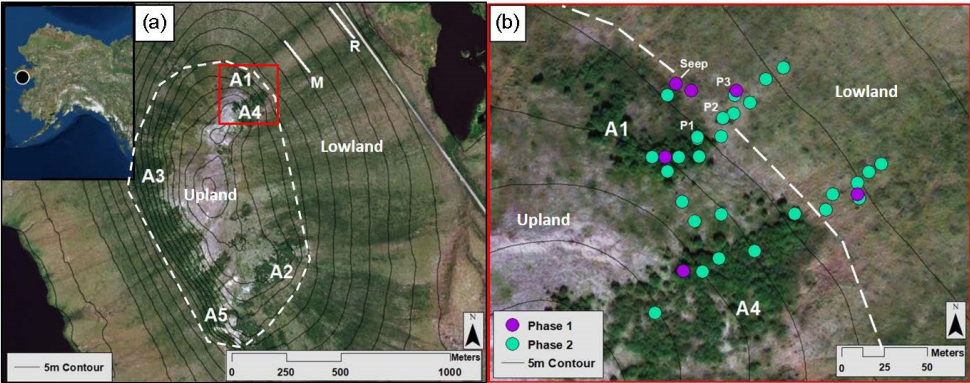
**Figure 1:** Kougarok Field Site and sampling locations. Upper left inset map with Kougarok Field Site denoted by a black circle, located approximately 80 kilometers inland from the town of Nome on the Seward Peninsula, AK. (a) Alder patch and transect locations at the Kougarok Hillslope. Solid white lines represent Middle (M) and Road (R) sampling transects. Dashed white line represents the boundary

between upland area and lowland area. (b) Higher resolution spatial sampling locations within A1 and A4 transects; corresponds to the red box in Fig. 1a. Phase 1 (July 2017) locations are denoted with purple dots. Green dots indicate additional locations sampled during Phase 2 (September 2017, July 2018, and September 2018). P1, P2, and P3 indicate Pit locations dug in July 2018. Dashed white line represents the boundary between upland area and lowland area. Aerial imagery in this figure are sourced from Esri, DigitalGlobe, GeoEye, Earthstar Geographics, CNES/Airbus DS, USDA, USGS, AeroGRID, IGN, and the GIS User Community.
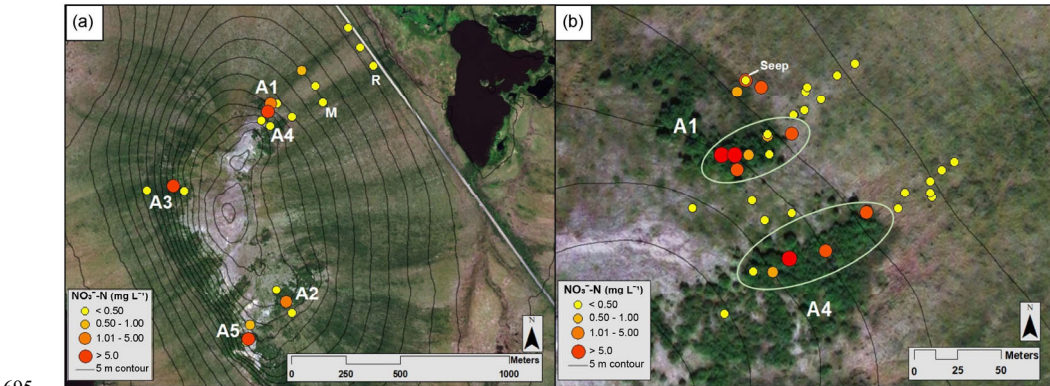
695

**Figure 2:** Map of mean NO$_3$-N concentrations from the Phase 1 and 2 sampling locations where yellow indicates low concentrations and red indicates high concentrations (see Key for ranges, scales differ slightly). (a) Circles represent NO$_3$-N concentrations at locations along the A1–A5, Middle, and Road transects in July 2017. (b) Dots represent average NO$_3$-N concentrations along the A1 and A4 transects and between the transects over all sampling campaigns. The green ellipses indicate samples collected *within* the alder shrubland, as opposed to *outside* the alder shrubland. Aerial imagery in this figure are sourced from Esri, DigitalGlobe, GeoEye, Earthstar Geographics, CNES/Airbus DS, USDA, USGS, AeroGRID, IGN, and the GIS User Community.

700
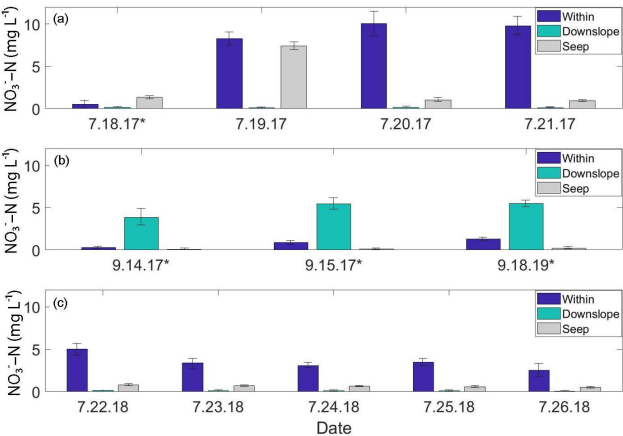
**Figure 3:** Soil pore water $NO_3^-$-N time series plots from the A1 transect. 'Within' and 'Downslope' denote sample locations within and downslope of shrublands along the transect; 'Seep' denotes a seep in the ground located on the A1 transect at the transition between upland and lowland. Standard deviations are displayed as black brackets on each bar. (a) July 2017 daily $NO_3^-$-N concentrations. (b) September 2017 daily $NO_3^-$-N concentrations. (c) July 2018 daily $NO_3^-$-N concentrations. Days marked with an asterisk (*) indicate precipitation events.

710
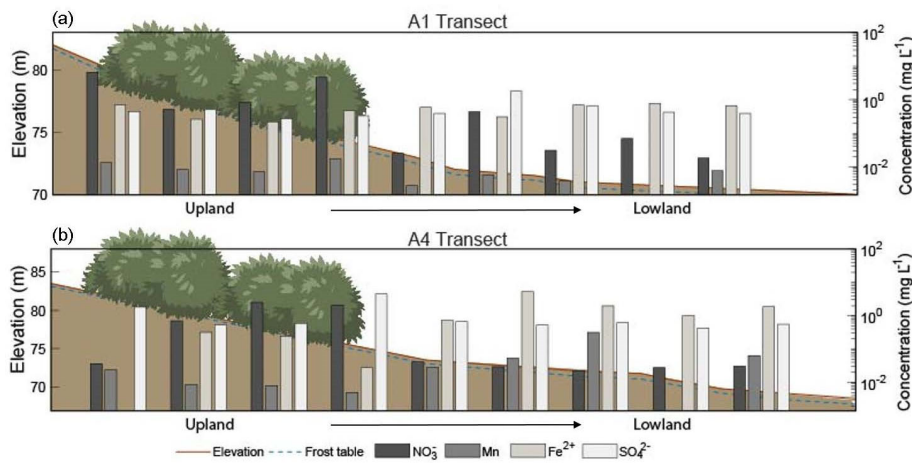
**Figure 4:** Elevation profiles and chemical concentrations along (a) A1 and (b) A4 transects, extending from the upland area to the lowland area during July (2018) sampling. Each sampling rhizon nest (depicted as histograms in these transects) is spaced ~10 m apart. Note that the elevation scale is different for A1 and A4 transects. Horizontal axis and shrubs not to scale. Depth to frozen soil or bedrock is depicted by the blue dashed line and shrubs indicate sample sites located within the alder shrubland. Redox species: nitrate ($NO_3^-$-N), manganese (Mn), iron ($Fe^{2+}$), and sulfate ($SO_4^{2-}$) are plotted along the secondary y-axis. See Tables S5-S6 in the associated Supplemental material for corresponding concentrations, n-values, and statistics.

715